

Color Doppler Aliasing: Unmasking the Diagnosis of Cardiac Rosai-Dorfman



Daniel Shirvani, BSc, Jong Moo Kim, MD, MHSc, Jaelyn Lam, BSc,
Michael Yin-Cheung Tsang, MD, Darwin Yeung, MD, Joel Price, MD, and
Christina Luong, MD, MHSc, Vancouver, British Columbia, Canada

INTRODUCTION

Cardiac masses are often detected on echocardiography as abnormal echodensities within the cardiac chambers. We report a case of a cardiac mass that was first identified on echocardiogram due to aliasing of color-flow Doppler of the pulmonary veins (PVs). This resulted in a cascade of testing that ultimately led to a diagnosis of Rosai-Dorfman disease (RDD). This rare condition is characterized by nonmalignant proliferation of histiocytes¹; RDD most often presents as painless cervical lymphadenopathy but presents a unique diagnostic challenge when confined to extranodal sites, especially in the heart. Cardiac involvement in RDD (cRDD) is exceedingly rare, making this case an important addition to the limited literature and highlighting the importance of acquiring additional views when unexpected findings arise during echocardiographic scanning.

CASE PRESENTATION

A 62-year-old woman of Asian descent presented to the emergency department with subacute worsening of atypical chest pain. In the emergency department, they were found to be in atrial flutter at a heart rate of 103 beats per minute with nonspecific ST-segment abnormalities. The physical exam did not reveal volume overload or findings suggestive of significant valve disease. Serial troponin and CK levels were normal. The patient spontaneously converted to sinus rhythm during the emergency department stay. Chest pain was deemed secondary to atrial flutter with rapid ventricular response, and they were discharged home with a referral to the rapid access cardiology clinic.

The patient was reassessed in the outpatient cardiology clinic where they were prescribed beta-blockers and apixaban and underwent an outpatient pharmacologic myocardial perfusion scan that was negative for myocardial ischemia with normal left ventricular systolic function. A 24-hour ambulatory electrocardiogram demonstrated paroxysmal atrial flutter with controlled ventricular response. A transthoracic echocardiogram (TTE) was performed to assess cardiac structure in the setting of newly diagnosed atrial flutter.

From the Faculty of Medicine (D.S.), Division of Cardiac Surgery (J.M.K., J.P.), and Division of Cardiology (J.L., M.Y.-C.T., D.Y., C.L.), University of British Columbia, Vancouver, British Columbia, Canada.

Keywords: Echocardiogram, Pulmonary vein stenosis, Cardiac mass

Correspondence: Dr. Christina L. Luong, MD, MHSc, University of British Columbia; Diamond Health Care Centre, 9th Floor Cardiology, 2775 Laurel Street, Vancouver, British Columbia V5Z 1M9, Canada (E-mail: christina.luong@ubc.ca).

Crown Copyright 2024. Published by Elsevier Inc. on behalf of the American Society of Echocardiography. This is an open access article under the CC BY-NC-ND license (<http://creativecommons.org/licenses/by-nc-nd/4.0/>).

2468-6441

<https://doi.org/10.1016/j.case.2024.04.007>

376

VIDEO HIGHLIGHTS

Video 1: Two-dimensional TTE, apical 4-chamber view with color-flow Doppler, demonstrates color-flow aliasing from a right PV.

Video 2: Transthoracic echocardiogram revealing abnormal two-dimensional TTE, apical 5-chamber view with color-flow Doppler, demonstrates color-flow aliasing from a right PV.

Video 3: Two-dimensional TTE, apical long-axis view with color-flow Doppler, demonstrates color-flow aliasing from a right pulmonary vein.

Video 4: Two-dimensional TTE, subcostal dual-display view without (*left*) and with (*right*) color-flow Doppler (midvalue Nyquist limit), demonstrates color-flow Doppler aliasing from a right pulmonary vein.

Video 5: Intraoperative two-dimensional transesophageal echocardiogram (TEE), midesophageal biplane, bicaval long-axis (*left*) and short-axis (*right*) view, demonstrates a mass at the interatrial septum in cross plane.

Video 6: Intraoperative two-dimensional TEE, midesophageal rightward rotated, long-axis (117°) view with color-flow Doppler (reduced Nyquist limit), demonstrates a mass encasing the right superior pulmonary veins with extension into the interatrial septum causing color-flow aliasing.

Video 7: Intraoperative two-dimensional TEE, midesophageal rightward rotated, long-axis (103°) view with color-flow Doppler, demonstrates color-flow aliasing from the right superior pulmonary vein stenosis due to a mass at the interatrial septum.

View the video content online at www.cvcasejournal.com.

The TTE showed normal biventricular systolic function and a moderately dilated left atrium (LA; 43 mL/m²) with no significant valve disease. Estimated pulmonary artery systolic pressure was 28 mm Hg. There was unexpected color-flow Doppler aliasing noted within the LA at the level of the PVs (Figure 1, Videos 1-4). Interrogation of the PV pulsed-wave Doppler flow demonstrated elevated velocities up to 1.4 m/sec of unclear significance. Multimodality imaging to further characterize cardiac structure was recommended.

While awaiting additional imaging the patient developed new exercise-limiting dyspnea. The subsequent cardiac computed tomography (CT) scan revealed thickening of the left atrial wall between the right superior and inferior PVs, as well as the atrial septum, measured at 18 mm in thickness. There was less extensive thickening of the superior dorsal and inferior LA (5-9 mm), with mild narrowing of the right

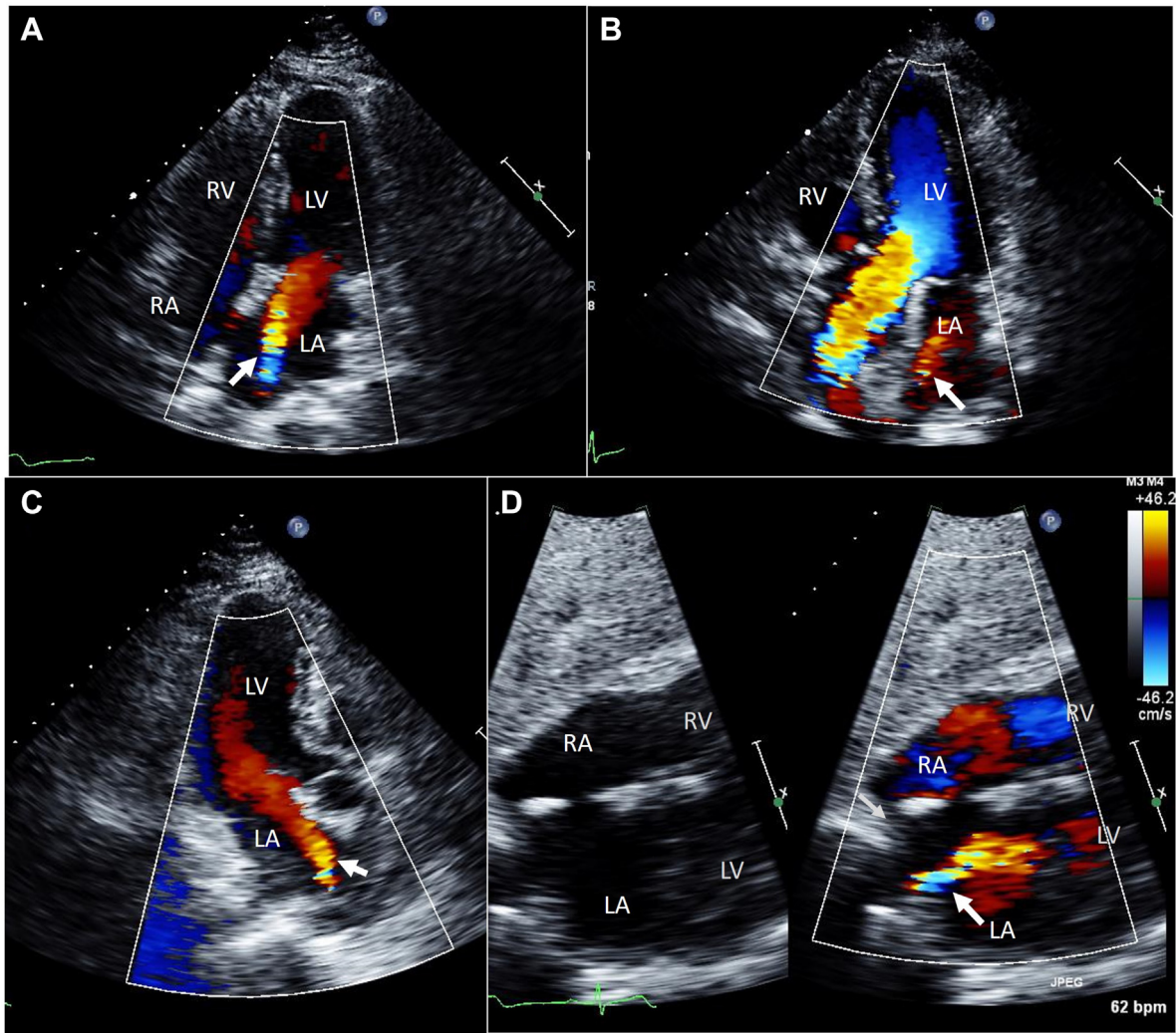


Figure 1 Two-dimensional TTE, apical 4-chamber (A), 5-chamber (B), and long-axis (C) views with color-flow Doppler, and subcostal dual-display view (D) without (left) and with (right) color-flow Doppler, demonstrates color-flow aliasing (arrows) from a right PV. LV, Left ventricle; RA, right atrium; RV, right ventricle.

superior and moderate stenosis of the right inferior PVs (Figure 2A). These findings were concerning for lymphoproliferative disorder, so a cardiovascular magnetic resonance scan was ordered. That scan revealed a soft tissue mass arising from the base of the LA and interatrial septum encasing and stenosing the right-sided PVs, impacting the right atrium and superior vena cava inflow (Figure 2B); however, no specific diagnoses could be made.

Given the concern for malignancy, the patient underwent comprehensive imaging, including CT scans of the head, chest, and abdomen, which were negative for other masses. A fludeoxyglucose-18 (FDG) positron emission tomography scan confirmed that the left atrial mass was intensely FDG avid, in keeping with possible malignancy (Figure 2C). No suspicious FDG-avid lesion was identified elsewhere. At this point the working diagnosis was for sarcoma or lymphoma; however, tissue confirmation was essential for management. No percutaneous options were feasible, and they were referred for open biopsy and mass resection.

Intraoperative transesophageal echocardiography guided the procedure (Figure 3, Videos 5-7). The mass was localized to the posterior left atrial wall, causing significant obstruction of the right inferior PV,

and there was mass effect at the cavoatrial junction (at the level of the inferior vena cava). The integration of the mass into the left atrial wall did not allow for significant resection, and a sample was taken for tissue diagnosis. Due to alterations in volume status during the surgery the mass caused obstruction of the inferior vena cava requiring transition from cardiopulmonary bypass to extracorporeal membrane oxygenation support. The patient remained on support for nearly 2 weeks and ultimately required a cavoatrial shunt for successful wean from support.

The tissue sample hematoxylin and eosin-stained sections showed myocardial tissue containing dense and destructive lymphoplasmacytic and histiocytic infiltrate mixed with areas of dense sclerosis. Lymphocytes were a mix of CD20+ PAX5+ B-cells and CD3+ T cells in a reactive distribution. Lymphocytes were positive for BCL2 and negative for BCL6. CD138 highlights abundant plasma cells, which are polytypic for kappa and lambda light chains. There was no significant increase in IgG4 staining relative to IgG staining. Histological findings were consistent with RDD.

The patient was diagnosed with extranodal RDD, exclusively in the heart. The patient underwent 4 infusions of rituximab over the course

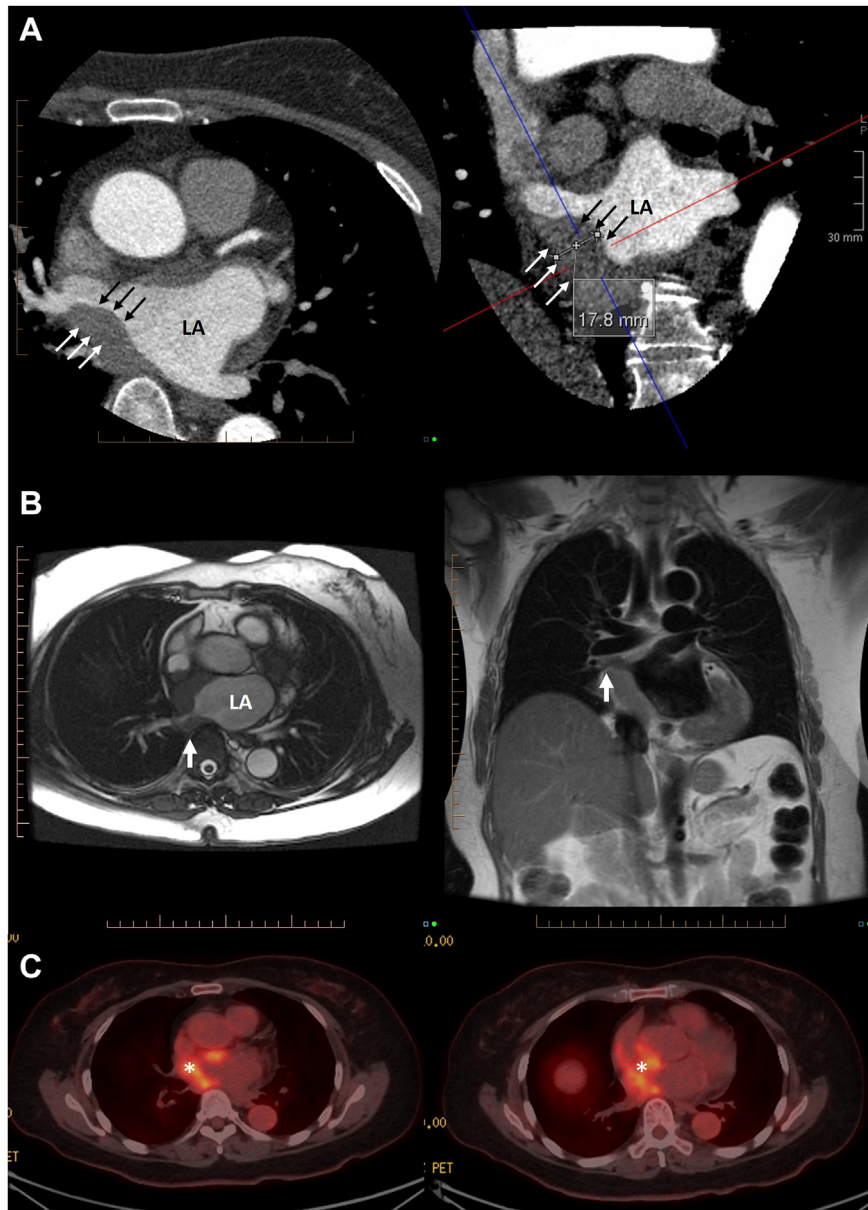


Figure 2 Multimodality imaging for evaluation of precise anatomic mass location and metabolic activity. **(A)** Cardiac CT, axial (*left*) and multiplanar oblique coronal (*right*) displays, demonstrates a poorly demarcated focal thickening of the posterior LA (*arrows*), between the right superior and inferior PVs and interatrial septum, measuring up to 18 mm, resulting in mild narrowing of the right superior and moderate stenosis of the right inferior PVs. **(B)** Cardiovascular magnetic resonance scan, balanced steady-state free precession axial display (*left*) and black-blood spin-echo sequence coronal display (*right*), demonstrates a soft tissue mass (isointense relative to the myocardium) encasing and stenosing the right-sided PVs (*arrows*) with encroachment on the superior vena cava. **(C)** Positron emission tomography with 198.6 MBq of FDG, superior (*left*) and midventricular (*right*) axial displays, demonstrates that the asymmetric left atrial wall thickening was intensely FDG avid (*).

of 4 weeks. Imaging with positron emission tomography at 1 month posttreatment demonstrated significant response with decreased FDG activity in the interatrial region, which could correspond with postsurgical inflammation. A cardiac CT scan 3 months posttreatment demonstrated decreased LA thickening (9 mm) with slight improvement in right-sided PV stenosis. At 6 months postoperatively they had improved from a clinical point of view and were ambulating short distances without walking aids, although they were not quite back to

baseline, with residual dyspnea on exertion. The hematology care team was satisfied with the patient's progress and planned to conduct radiological studies every 3 to 6 months to reevaluate the atrial mass.

DISCUSSION

Rosai-Dorfman disease is an idiopathic nonmalignant proliferation of non-Langerhans sinus histiocytes,¹⁻³ which often presents as painless,

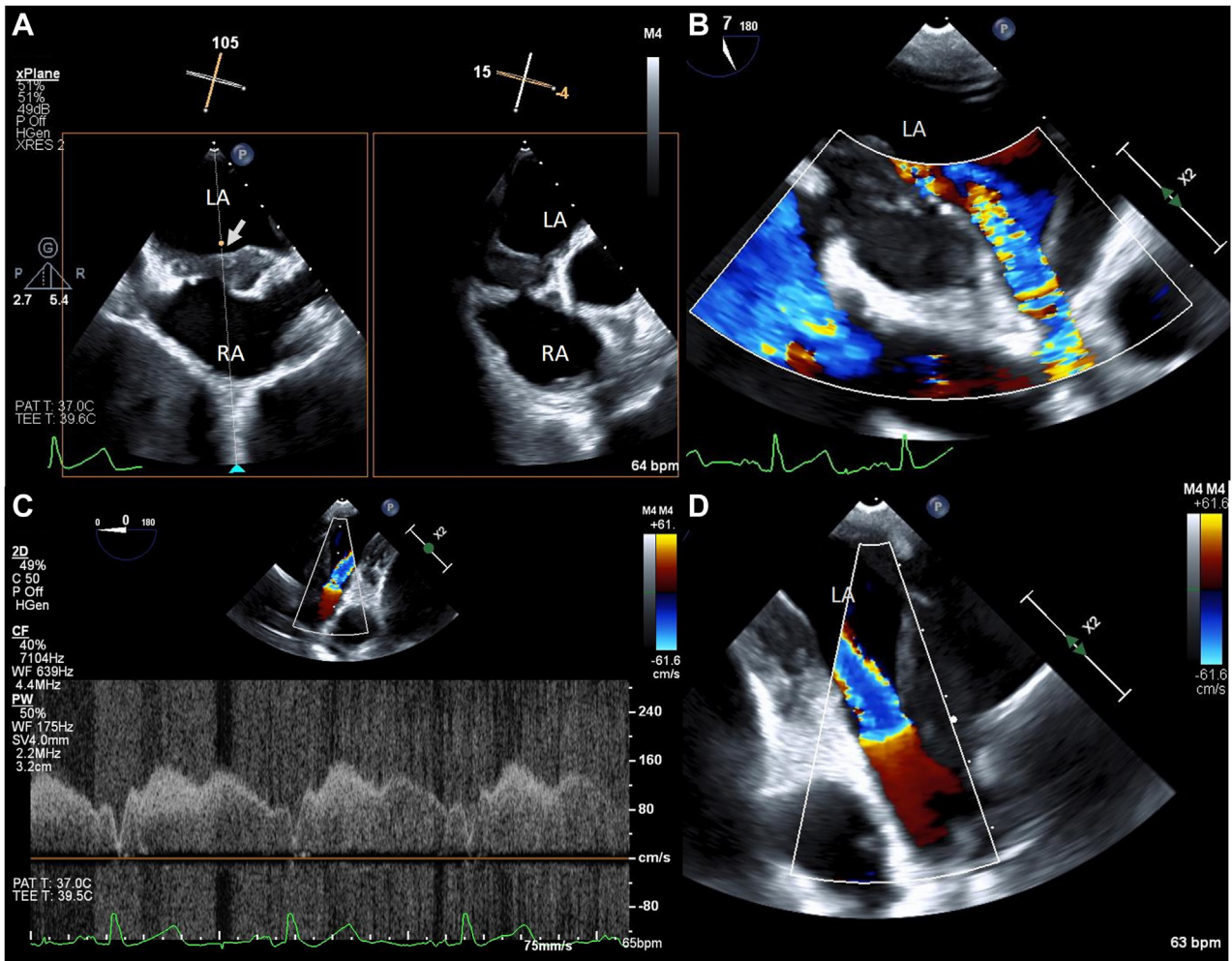


Figure 3 Intraoperative two-dimensional transesophageal echocardiogram, bicaval biplane **(A)** long-axis (*left*) and short-axis (*right*) view, demonstrates a mass (*arrow*) at the interatrial septum in cross plane; **(B)** rightward rotated, long-axis (117°) view with reduced Nyquist color-flow Doppler and **(D)** long-axis (103°) view with normal scale color-flow Doppler, demonstrates right superior PV stenosis; **(C)** short-axis display (0°) with color-flow Doppler-guided pulsed-wave spectral Doppler, demonstrates a pathologic continuous flow pattern and increased maximal systolic velocity at 1.6 m/sec.

massive bilateral cervical lymphadenopathy in young adults and children. The disease is very rare, with an incidence of about 3 per million, with approximately 1,000 cases having been reported in literature.² However, RDD is generally self-limiting and does not threaten life.^{1,4} Definitive diagnosis is done by histological assessment.⁵

Rosai-Dorfman disease with additional masses outside of the lymph nodes, known as extranodal RDD, is observed in 25% to 40% of cases.^{1,6} Due to nonspecific symptoms and a diverse range of mass sites, its presentation may closely resemble various inflammatory or neoplastic disorders, leading to potential misdiagnosis.² Extranodal-only presentations of RDD are very rare, and are significantly more difficult to treat and identify due to lack of common cervical symptoms.^{1,2} Additionally, the diagnosis of extranodal RDD may be complicated by excess fibrosis or emperipolesis, as compared with nodal RDD.¹

Cardiac involvement in RDD is extremely rare and is reported to occur in 0.1% to 0.2% of cases.⁵ Reported cases of cRDD masses have been found within the epicardium, pericardium, pulmonary artery, and 4 chambers with or without infiltration.^{5,7} The treatment and

prognosis of cRDD remains unknown. However, limited data, including a case series of 15 adults, suggest the most favorable outcomes were in patients for whom surgical excision was feasible.⁵ Our patient was unable to undergo surgical excision, which resulted in a requirement for cavoatrial bypass related to mass effect; however, since then, there has been radiographic response and improvement in clinical status.

The current patient represents a rarity among rarities: a case of extranodal-only cRDD. This condition was detected incidentally on a routine TTE for atrial flutter. During the TTE, there was unexpected color-flow Doppler aliasing at the PVs associated with elevated PV velocity. The astute sonographer identified the abnormality at the time of scanning and augmented the views through off-axis windows.

The finding of turbulent PV flow on color-flow Doppler should raise suspicion of PV stenosis with flow velocities >1.1 m/sec indicating possible obstruction.⁸ Pulmonary vein stenosis may be congenital or acquired, with the latter often associated with radiofrequency ablation procedures as well as less common extrinsic processes such as neoplasms, sarcoidosis, or fibrosing mediastinitis.⁹⁻¹¹ Due to the

suspicious TTE, our patient underwent additional imaging, and subsequent biopsy revealed the definitive diagnosis of extranodal-only cRDD.

CONCLUSION

This patient is an exceedingly rare case of cardiac-isolated RDD. This report underscores the complexity of diagnosing cardiac masses, given that rare disease may mimic more common cardiac pathologies. The diagnostic journey, involving a combination of imaging modalities and histopathological analysis, highlights the necessity of an integrated approach in cardiac care. This case contributes to the limited literature on extranodal-only cRDD, providing valuable insights for future similar cases. The successful identification and treatment of this rare disease also demonstrate the evolving capabilities of cardiac imaging and surgical techniques.

ETHICS STATEMENT

The authors declare that the work described has been carried out in accordance with The Code of Ethics of the World Medical Association (Declaration of Helsinki) for experiments involving humans.

CONSENT STATEMENT

Complete written informed consent was obtained from the patient (or appropriate parent, guardian, or power of attorney) for the publication of this study and accompanying images.

FUNDING STATEMENT

This research did not receive any specific grant from funding agencies in the public, commercial, or not-for-profit sectors.

DISCLOSURE STATEMENT

The authors report no conflicts of interests.

ACKNOWLEDGMENTS

We thank Dr. Duncan Ferguson for providing expertise and assistance with image extraction related to the cardiovascular magnetic

resonance, cardiac computed tomography, and positron emission tomography scans.

SUPPLEMENTARY DATA

Supplementary data related to this article can be found at <https://doi.org/10.1016/j.case.2024.04.007>.

REFERENCES

1. Bruce-Brand C, Schneider JW, Schubert P. Rosai-Dorfman disease: an overview. *J Clin Pathol* 2020;73:697-705.
2. Yontz LA, Franco A, Sharma S, Lewis KN, McDonough CH. A case of Rosai-Dorfman Disease in a pediatric patient with cardiac involvement. *J Radiol Case Rep* 2012;6:1-8.
3. Tsigaridas N, Mantzoukis S, Mpakas K, Troganis E, Patsouras D. A rare case of cardiac involvement in rosai-dorfman disease. *J Cardiovasc Imaging* 2019;27:286.
4. Azari-Yaam A, Abdolsalehi MR, Vasei M, Safavi M, Mehdizadeh M. Rosai-dorfman disease: a rare clinicopathological presentation and review of the literature. *Head Neck Pathol* 2021;15:352-60.
5. O'Gallagher K, Dancy L, Sinha A, Sado D. Rosai-Dorfman disease and the heart. *Intractable Rare Dis Res* 2016;5:1-5.
6. Maleszewski JJ, Hristov AC, Halushka MK, Miller DV. Extranodal Rosai-Dorfman disease involving the heart: report of two cases. *Cardiovasc Pathol* 2010;19:380-4.
7. Wang TKM, Mukherjee S, Tan CD, Shepard D, Pettersson G, Desai M. Rosai-dorfman disease of the right ventricular outflow tract: role of multimodality imaging. *Circ Cardiovasc Imaging* 2020;13:e010783.
8. Fadel BM, Pibarot P, Kazzi BE, Al-Admawi M, Galzerano D, Alhumaid M, et al. Spectral Doppler interrogation of the pulmonary veins for the diagnosis of cardiac disorders: a comprehensive review. *J Am Soc Echocardiogr* 2021;34:223-36.
9. Saad EB, Marrouche NF, Saad CP, Ha E, Bash D, White RD, et al. Pulmonary vein stenosis after catheter ablation of atrial fibrillation: emergence of a new clinical syndrome. *Ann Intern Med* 2003;138:634.
10. Den Bakker MA, Thomeer M, Maat APWM, Groeninx Van Zoelen CE. Life-threatening hemoptysis caused by chronic idiopathic pulmonary hilar fibrosis with unilateral pulmonary vein occlusion. *Ann Diagn Pathol* 2005;9:319-22.
11. Nunes H, Humbert M, Capron F, Brauner M, Sitbon O, Battesti JP, et al. Pulmonary hypertension associated with sarcoidosis: mechanisms, haemodynamics and prognosis. *Thorax* 2005;61:68-74.